

# Interplay between the charge density wave phase and a pseudogap under antiferromagnetic correlations

Leonardo Prauchner<sup>1\*</sup>, Eleonir Calegari<sup>2</sup>, Julian Faúndez<sup>1</sup>,  
Sergio Magalhaes<sup>1</sup>

<sup>1</sup>Instituto de Física, Universidade Federal do Rio Grande do Sul, 91501-970, Porto Alegre, RS, Brazil

<sup>2</sup>Departamento de Física - Universidade Federal de Santa Maria, 97105-900, Santa Maria, RS, Brazil

E-mail: leo.prauchner@gmail.com

## Abstract.

In this study, we explore the impact of short-range antiferromagnetic correlations on the charge density wave (CDW) phase in strongly correlated electron systems exhibiting the pseudogap phenomenon. Our investigation employs a  $n$ -pole approximation to consider the repulsive Coulomb interaction ( $U$ ) and antiferromagnetic correlations. Utilizing a two-dimensional Hubbard model for the Coulomb interaction and a BCS-like model for the CDW order parameter, we observe that an increase in  $U$  enhances antiferromagnetic fluctuations, resulting in a flattened re-normalized band around the anti-nodal point  $(\pi, 0)$ . The pseudogap manifests in the band structure and density of states, prompting an exploration across various  $U$  and occupation number values. Our findings indicate that antiferromagnetic correlations significantly influence the CDW state, as the Fermi surface is reconstructed within the ordered phase. Furthermore, we find a Lifshitz transition inside both the CDW phase and the normal state, with the latter preceding the onset of the pseudogap.

## 1. Introduction

The pseudogap (PG) is a very enigmatic, and yet, not fully understood phenomenon. Characterized by suppression of states around the Fermi level below a certain temperature  $T^*$  [1, 2], as well as a topological transition on the Fermi Surface (FS), which assumes a pocket-like shape [3, 4, 5, 6, 7, 8]. This phenomenon is generally observed in strongly correlated electron systems, such as the cuprates [9] and pnictides [10]. However, we can also highlight Selenium-based compounds, in particular, 1T-TaSe<sub>2</sub> [11], capable of showing both PG and charge density wave (CDW) [12] when the system is quasi-2D. In some cases, these compounds also have a superconducting order [13, 14, 15] displaying a phase diagram similar to the cuprates [16]. Additionally, we mention infinite-layered nickelates [17, 18], where the PG phenomenon is accompanied by the emergence of superconductivity and, eventually, CDW.

On the other hand, a plethora of mechanisms have been proposed to explain the onset and nature of the PG phenomenon [19, 20, 21, 22, 23, 24, 25, 26, 27, 28]. In cuprates, the short-range magnetic correlations due to the vicinity of the antiferromagnetic phase in the underdoped region can be of utmost importance to clarify the entire PG phenomenon. For instance, there is a change from the hole to electron-like FS topology, the so-called Lifshitz transition (LT). This transition happens when the system is still doped by holes. Moreover, this transition precedes the collapse of the FS to a pocket shape, characterizing the onset of the PG [29, 30, 31, 32]. Surprisingly, for temperatures below  $T^*$ , there is a CDW transition accompanied by a FS reconstruction [33, 34]. There is some evidence that short-range antiferromagnetic correlations may be present within the CDW [35, 36, 37, 38]. Thus, it is possible to speculate whether such correlations may be involved in this FS reconstruction. It is also important to highlight that the role of short-range antiferromagnetic correlations may not be exclusive to cuprates, since the same origin of PG is considered in nickelates [39]. The same scenario could be cogitated about the two-dimensional transition metal dichalcogenides (TMDs) since a Mott insulator behavior is observed [40]. Thus, a question arises: how short-range antiferromagnetic correlations can influence an interplay between the CDW and the entire PG phenomenon?

As a proposal to answer the question above, we start from a BCS-like mean field theory within the Green's function equation of motion formalism to describe the CDW instability. Then, we replace the normal state uncorrelated Green's function with a correlated one, obtained through the n-pole approximation [41], applied to the single-band Hubbard model [42]. That is a way to consider short-range antiferromagnetic correlations in the normal state. The n-pole approximation was proposed as a correction to the Hubbard-I approximation [43], which is unable to capture magnetic solutions and antiferromagnetic correlations. The limitation of the Hubbard I approximation is due to the absence of quantities such as the spin-spin correlation  $\langle \vec{S}_i \cdot \vec{S}_j \rangle$ , and the double occupation  $\langle N_i N_j \rangle$ . Those correlations compose the band shift ( $Y_{\vec{k},\sigma}$ ) which appears in the n-pole approximation. In our theory, we highlight the importance of the next nearest

neighbors hopping ( $t_1$ ). It plays a fundamental role along with the occupation number ( $n_T$ ) and the Coulomb interaction ( $U$ ), affecting  $Y_{\vec{k},\sigma}$  through  $\langle N_i N_j \rangle$  and mainly  $\langle \vec{S}_i \cdot \vec{S}_j \rangle$ , distorting the bands. As a consequence, there is a flattening of the band around the  $(\pi, 0)$  point, which originates a Van Hove singularity (VHS) and can favor pair formation and stabilize the CDW below a critical temperature ( $k_B T_C$ ) [44, 45, 46].

Besides, we shall demonstrate that the short-range antiferromagnetic fluctuations affecting  $Y_{\vec{k},\sigma}$  can also favor the opening of a PG. There is a displacement of accessible states to the VHS, causing suppression of states in adjacent energy regions [47, 48]. Moreover, the distortion of the bands eventually can cause a Lifshitz transition (LT) [49, 50, 51]. This scenario can be understood from the perspective of the density of states (DOS). The position of the VHS relative to the Fermi level reflects the change in the FS topology when it goes through it, changing from a hole-like topology (from lower energy levels) to an electron-like one. Indeed, the temperature effects are crucial in our theory since the shape of the DOS is affected by the VHS peak structure, which depends if the system is in a normal state, or within the ordered phase.

For this work, we chose a square lattice and set the CDW order form factor as an unconventional  $d$ -wave symmetry, in contrast with the usual  $s$ -wave gap symmetry that has been explored in some cuprates. In cuprates and TMDs, the CDW coexists with another competing order [52, 53], such as the superconductivity [54]. This choice of symmetry is not arbitrary, as both  $s$ -wave and  $d$ -wave cases have been observed [55, 56], and can even compete, making it difficult to determine the predominant form factor [57, 58]. However, we only investigated the  $d$ -wave symmetry case. Our theory does not necessarily assume a phononic mechanism for electron-hole pair formation. Indeed, several authors have suggested that strongly correlated electron systems may have different origins for the phase transition from the normal state to CDW [59, 60, 61, 62, 63].

This paper is organized as follows. The model, and the equations obtained with the chosen method, are presented in section 2. The numerical results are presented and discussed in section 3. Conclusions and further remarks are shown at the end.

## 2. Model

We studied the effects of antiferromagnetic correlations on the CDW phase, employing a BCS-like model [64]:

$$\mathcal{H} = \sum_{\vec{k}} \xi_{\vec{k}} \left[ c_{\vec{k},\uparrow}^\dagger c_{\vec{k},\uparrow} + c_{\vec{k},\downarrow}^\dagger c_{\vec{k},\downarrow} \right] + \sum_{\vec{k}} W_{\vec{k}} \left[ c_{\vec{k}+\vec{Q},\uparrow}^\dagger c_{\vec{k},\uparrow} + c_{\vec{k}+\vec{Q},\downarrow}^\dagger c_{\vec{k},\downarrow} \right] + H_0, \quad (1)$$

where  $W_{\vec{k}}$  is the CDW order parameter,  $\xi_{\vec{k}} = \varepsilon_{\vec{k}} - \mu = 2t_0(\cos k_x + \cos k_y) + 4t_1 \cos k_x \cos k_y - \mu$  is the square lattice quasi-particle dispersion relation,  $\mu$  is the chemical potential and  $H_0 = \sum_{\vec{k}} |W_{\vec{k}}|^2 / |V|$ . The CDW order parameter is obtained through the following relation:

$$W_{\vec{k}} = |V| \gamma_{\vec{k}} \sum_{\vec{k}'} \langle c_{\vec{k}+\vec{Q}',\sigma}^\dagger c_{\vec{k}',\sigma} \rangle, \quad (2)$$

$\gamma_{\vec{k}}$  is the  $d$ -wave symmetry factor and  $|V|$  is the attractive pairing potential absolute value. We propose that  $W_{\vec{k}}$  can model the CDW gap, as it represents the creation of an electron-hole pair, modulated by the nesting vector  $Q = (\pi, \pi)$ . We do not consider the Debye cutoff energy and a self-consistent non  $\vec{k}$ -dependent renormalizing term [64], since the pairing mechanism is not defined as phononic. The Hamiltonian can be written in the quadratic form as:

$$\mathcal{H} = \Psi^\dagger \mathcal{H}_{\vec{k}} \Psi + H_0, \quad (3)$$

where  $\Psi$  is a Nambu spinor, given by:

$$\Psi^\dagger = \left( c_{\vec{k},\uparrow}^\dagger \quad c_{-\vec{k},\downarrow} \quad c_{\vec{k}+\vec{Q},\uparrow}^\dagger \quad c_{-\vec{k}+\vec{Q},\downarrow} \right). \quad (4)$$

The coefficients matrix  $\mathcal{H}_{\vec{k}}$  is needed, and was obtained through the use of Green's functions in the Zubarev's formalism [65], whose equation of motion is:

$$\omega \langle \langle \hat{A}; \hat{B} \rangle \rangle = \langle [\hat{A}, \hat{B}]_+ \rangle + \langle \langle [\hat{A}, \mathcal{H}]; \hat{B} \rangle \rangle. \quad (5)$$

We can apply the last equation to the set of operators, starting with  $\langle \langle c_{\vec{k},\uparrow}^\dagger; c_{\vec{k},\uparrow}^\dagger \rangle \rangle$ :

$$\omega \langle \langle c_{\vec{k},\uparrow}^\dagger; c_{\vec{k},\uparrow}^\dagger \rangle \rangle = 1 + \xi_{\vec{k}} \langle \langle c_{\vec{k},\uparrow}^\dagger; c_{\vec{k},\uparrow}^\dagger \rangle \rangle + W_{\vec{k}+\vec{Q}} \langle \langle c_{\vec{k}+\vec{Q},\uparrow}^\dagger; c_{\vec{k},\uparrow}^\dagger \rangle \rangle, \quad (6)$$

and repeating the procedure for the remaining operators, results in the coefficients matrix  $\mathcal{H}_{\vec{k}}$ :

$$\mathcal{H}_{\vec{k}} = \begin{pmatrix} \xi_{\vec{k}} & 0 & W_{\vec{k}} & 0 \\ 0 & -\xi_{\vec{k}} & 0 & -W_{\vec{k}} \\ W_{\vec{k}+\vec{Q}} & 0 & \xi_{\vec{k}+\vec{Q}} & 0 \\ 0 & -W_{\vec{k}+\vec{Q}} & 0 & -\xi_{\vec{k}+\vec{Q}} \end{pmatrix}. \quad (7)$$

Thus, the equation of motion for the Green's function matrix  $\mathcal{G}(\vec{k}, \omega)$ , whose elements are given by  $\mathcal{G}_{l,s} = \langle \langle \hat{A}_l; \hat{B}_s \rangle \rangle$ , can be solved, with  $\mathcal{I}$  as a fourth-order identity matrix.

$$(\omega \mathcal{I} - \mathcal{H}_{\vec{k}}) \mathcal{G}(\vec{k}, \omega) = \mathcal{I}. \quad (8)$$

In the normal state,  $W_{\vec{k}} = 0$ , so we define a new quantity, corresponding to the ground state uncorrelated Green's function  $G_0(\vec{k}, \omega)$ :

$$G_0(\vec{k}, \omega) = (\omega - \xi_{\vec{k}})^{-1}. \quad (9)$$

This new quantity appears in the main diagonal of  $\mathcal{G}(\vec{k}, \omega)$ , so we rewrite it, which allows us to reevaluate the coefficients matrix.

$$\mathcal{G}(\vec{k}, \omega) = \begin{pmatrix} G_0^{-1}(\vec{k}, \omega) & 0 & -W_{\vec{k}} & 0 \\ 0 & G_0^{-1}(\vec{k}, \omega) & 0 & -W_{\vec{k}} \\ -W_{\vec{k}+\vec{Q}} & 0 & G_0^{-1}(\vec{k}+\vec{Q}, \omega) & 0 \\ 0 & -W_{\vec{k}+\vec{Q}} & 0 & G_0^{-1}(\vec{k}+\vec{Q}, \omega) \end{pmatrix}^{-1}. \quad (10)$$

At this point, we replace the Green's function  $G_0(\vec{k}, \omega)$  by a normal state correlated Green's function obtained through the n-pole approximation applied to the single-band Hubbard model [42]. The single-band Hubbard model is given as:

$$\mathcal{H} = \sum_{\langle\langle i,j,\sigma \rangle\rangle} t_{ij} c_{i,\sigma}^\dagger c_{j,\sigma} + U \sum_{i,\sigma} n_{i,\sigma} n_{i,-\sigma}, \quad (11)$$

where  $t_{ij}$  is the hopping amplitude,  $n_{i,\sigma} = c_{i,\sigma}^\dagger c_{i,\sigma}$  is the occupation number operator with spin  $\sigma = \{\uparrow, \downarrow\}$ ,  $U$  is the local repulsive Coulomb interaction and the  $\langle\langle \dots \rangle\rangle$  symbol indicates a sum over first and second nearest neighbors. We highlight that within the n-pole approximation, the second nearest neighbor hopping is crucial to properly capture the short-range antiferromagnetic correlation effects that give rise to the PG phenomenon. Additionally, to address the infinite chain of Green's functions given by the equation of motion applied to the Hubbard model, a finite set of relevant operators  $\{A_n\} = \{c_{i,\sigma}, n_{i,-\sigma} c_{i,\sigma}, c_{j,\sigma}^\dagger, n_{j,-\sigma} c_{j,\sigma}^\dagger\}$  is defined, capable of linearizing equation (5), giving rise to the correlated Green's functions matrix:

$$\mathbf{G}(\vec{k}, \omega) = \mathbf{N}(\omega \mathbf{N} - \mathbf{E}(\vec{k}))^{-1} \mathbf{N}, \quad (12)$$

with  $N_{nm} = \langle [\hat{A}_n, \hat{A}_m^\dagger]_+ \rangle$  and  $E_{nm} = \langle [[\hat{A}_n, \mathcal{H}], \hat{A}_m^\dagger]_+ \rangle$ . Solving the last equation results in the correlated Green's function matrix. One of the most important elements is given by:

$$G_{11,\sigma}(\omega, \vec{k}) = \frac{\omega - U(1 - n_\sigma) - Y_{\vec{k},\sigma}^-}{(\omega - \varepsilon_{\vec{k}})(\omega - U - Y_{\vec{k},\sigma}^-) - U n_\sigma (\varepsilon_{\vec{k}} - Y_{\vec{k},\sigma}^-)}, \quad (13)$$

where  $Y_{\vec{k},\sigma}$  is the band shift. This quantity is significant, as it contains all of the antiferromagnetic correlation effects, responsible for the opening of the PG. The shift causes the energy bands to be displaced towards energy levels below the Fermi level. This effect is much stronger in the region close to the nodal point  $(\pi, \pi)$ , but also affects the anti-nodal points, such as  $(\pi, 0)$ , where the PG is opening. Therefore,  $Y_{\vec{k},\sigma}$  is defined as:

$$\langle n_{-\sigma} \rangle (1 - \langle n_{-\sigma} \rangle) Y_{\vec{k},\sigma}^- = \Gamma_\sigma^{(0)} + \sum_{j \neq i} e^{i\vec{k} \cdot (\vec{R}_i - \vec{R}_j)} t_{ij} (\Gamma_{i,j,\sigma}^{(1)} + \Gamma_{i,j,\sigma}^{(2)} + \Gamma_{i,j,\sigma}^{(3)}), \quad (14)$$

with the components  $\Gamma_{i,j,\sigma}^m$  given by the following terms:

$$\Gamma_\sigma^{(0)} = - \sum_{j \neq i} t_{ij} \langle c_{i,\sigma}^\dagger c_{j,\sigma} (1 - n_{i,-\sigma} - n_{j,-\sigma}) \rangle, \quad (15)$$

$$\Gamma_{i,j,\sigma}^{(1)} = \frac{1}{4}(\langle N_i N_j \rangle - \langle N_j \rangle \langle N_i \rangle), \quad (16)$$

$$\Gamma_{i,j,\sigma}^{(2)} = \langle \vec{S}_i \cdot \vec{S}_j \rangle, \quad (17)$$

and

$$\Gamma_{i,j,\sigma}^{(3)} = -\langle c_{j,\sigma}^\dagger c_{j,-\sigma}^\dagger c_{i,-\sigma} c_{i,\sigma} \rangle, \quad (18)$$

where  $N_i = n_{i,\sigma} + n_{i,-\sigma}$  being the total occupation operator per site. When short-range antiferromagnetic correlations cause the PG, the momentum dependence of  $Y_{\vec{k},\sigma}$  is essential to capture this phenomenon [66]. Then, the inverse Fourier transform of  $\Gamma_{i,j,\sigma}^m$  is taken to reintroduce this dependence into  $Y_{\vec{k},\sigma}$ .

$$\Gamma_{i,j,\sigma}^{(m)} = \frac{1}{L} \sum_{\vec{q}} e^{-i\vec{q} \cdot (\vec{R}_j - \vec{R}_i)} \Gamma_{\vec{q},\sigma}^{(m)}. \quad (19)$$

For this approach, we need the quasi-particle dispersion relation, given by:

$$\varepsilon(\vec{k} - \vec{q}) = \frac{1}{L} \sum_{j \neq i} e^{i(\vec{k} - \vec{q}) \cdot (\vec{R}_j - \vec{R}_i)} t_{ij}, \quad (20)$$

now, it is possible to define a new compact form for  $Y_{\vec{k},\sigma}$ :

$$\langle n_{-\sigma} \rangle (1 - \langle n_{-\sigma} \rangle) Y_{\vec{k},\sigma} = \Gamma_{\sigma}^{(0)} + \sum_{\vec{q}, m=1,3} \varepsilon(\vec{k} - \vec{q}) \Gamma_{\vec{q},\sigma}^{(m)}. \quad (21)$$

With the last definition,  $Y_{\vec{k},\sigma}$  has a non-uniform structure in the momentum space, which implies a band distortion, leading to a PG similar to that observed in cuprates. By solving equation (8), we obtain the polynomial given by the determinant of the coefficients matrix, whose poles are the energy bands. The polynomial is written as:

$$P(\vec{k}, \omega) = G_{11,\downarrow}^{-1}(\vec{k}, \omega) G_{11,\uparrow}^{-1}(\vec{k}, \omega) G_{11,\downarrow}^{-1}(\vec{k} + \vec{Q}, \omega) G_{11,\uparrow}^{-1}(\vec{k} + \vec{Q}, \omega) \\ - [G_{11,\downarrow}^{-1}(\vec{k}, \omega) G_{11,\downarrow}^{-1}(\vec{k} + \vec{Q}, \omega) - G_{11,\uparrow}^{-1}(\vec{k}, \omega) G_{11,\uparrow}^{-1}(\vec{k} + \vec{Q}, \omega)] W_{\vec{k}}^2 + W_{\vec{k}}^4, \quad (22)$$

where we replaced  $G_0(\vec{k}, \omega)$  by the correlated normal state Green's function  $G_{11,\sigma}(\vec{k}, \omega)$  defined in equation (13). Through such replacement, besides the correlations, an explicit spin dependence is also included. For practicality, the Green's functions are separated in partial fractions, as it explicitly shows the form factors of the spectral weights, which are extremely relevant for the study of the quantities of interest. Thus, the general form for these Green's functions is defined below, with  $z_{m,\sigma}$  as the poles of  $P(\vec{k}, \omega)$ , which is the determinant of the coefficients matrix.

$$\mathcal{G}_{ls,\sigma}(\vec{k}, \omega) = \sum_{m=1,4} \frac{Z_{m,\sigma}^{ls}(\vec{k})}{(\omega - z_{m,\sigma})}, \quad (23)$$

where  $Z_{m,\sigma}^{ls}$  are the spectral weights of the Green's function. Moreover, we define  $\Lambda_{\sigma}^{ls}(\vec{k})$  as the numerator of the Green's function  $\mathcal{G}_{ls,\sigma}(\vec{k}, \omega)$ , resulting in:

$$Z_{n,\sigma}^{ls}(\vec{k}) = \frac{\Lambda_{\sigma}^{ls}(\vec{k})}{\prod_{m \neq n}^{m=1,4} (z_{n,\sigma} - z_{m,\sigma})}. \quad (24)$$

The choice of this representation for Green's functions facilitates the calculation of correlation functions. The most relevant Green's functions for this work is  $\mathcal{G}_{11,\sigma}(\vec{k}, \omega)$ , associated with the occupation number, the DOS, and the spectral function. Furthermore,  $\mathcal{G}_{13,\sigma}(\vec{k}, \omega)$  enables the order parameter calculation.

To evaluate the correlation functions, we use the standard integration, where the contour encircles the real axis without enclosing the poles of the Fermi function  $\eta_F(\omega)$ . Thus, the correlation functions are given by:

$$\langle \hat{B} \hat{A} \rangle = \oint \langle \langle \hat{A}; \hat{B} \rangle \rangle \eta_F(\omega) d\omega, \quad (25)$$

and applying that representation to  $\mathcal{G}_{11,\sigma}(\vec{k}, \omega)$ , results in the occupation number:

$$\langle n_{\sigma} \rangle = \frac{1}{N} \sum_{\vec{k}} \sum_{m=1,4} Z_{m,\sigma}^{11}(\vec{k}) \eta_F(z_{m,\sigma}). \quad (26)$$

Repeating the process for  $\mathcal{G}_{13,\sigma}(\vec{k}, \omega)$ :

$$W_{\vec{k}} = \frac{1}{N} |V| \gamma_{\vec{k}} \sum_{\vec{k}'} \sum_{m=1,4} Z_{m,\sigma}^{13}(\vec{k}') \eta_F(z_{m,\sigma}). \quad (27)$$

### 3. Numerical Results

To ensure all of the results are consistent, we use  $|t_0| = 1.0$  eV as the energy unit, and  $|V| = 1.2|t_0|$ .

The primary goal of this study is to demonstrate the connection between the impact of short-range antiferromagnetic correlations and the reconstruction of the FS within the CDW phase. We aim to elucidate the connection between this phenomenon and the emergence of the PG. The band shift  $Y_{\vec{k},\sigma}$  having a structure on the momentum space leads to a distortion on the nodal point  $(\pi, \pi)$ , as well as in the anti-nodal point  $(\pi, 0)$ . The distortions are enhanced by second nearest neighbors hopping  $t_1$  and characterized as a displacement of the bands towards lower energies, that when sufficiently intense, allow the reconstruction of the FS, and can lead to the opening of a PG. To analyze the relevance of antiferromagnetic correlations in the CDW phase, energy bands were obtained through the spectral function, calculated along the high-symmetry regions of the first Brillouin zone. Analyzing the bands from this perspective allows for visualizing the contribution of each band component to the system.

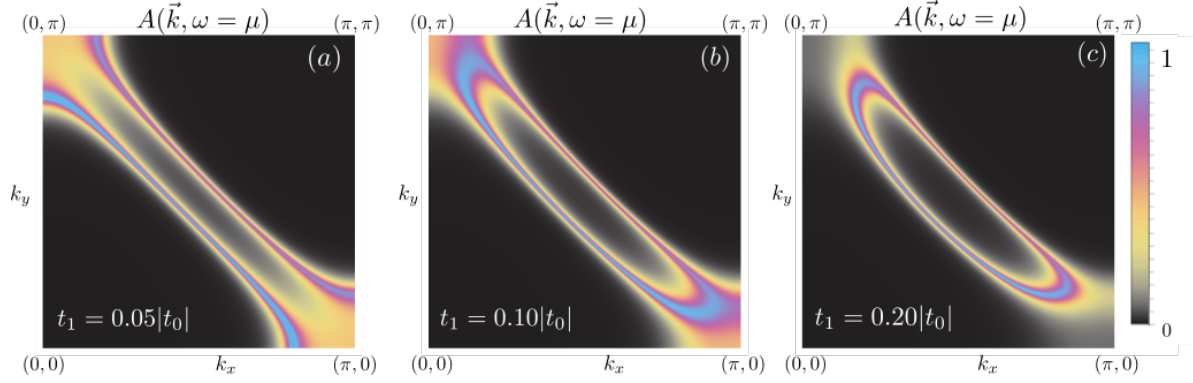


**Figure 1.** Fermi surfaces in the normal state with  $U = 9.0|t_0|$ ,  $n_T = 0.90$ ,  $k_B T = 0.05|t_0|$  for (a)  $t_1 = 0.05|t_0|$ , (b)  $t_1 = 0.10|t_0|$  and (c)  $t_1 = 0.20|t_0|$ . In panel (c), the Fermi surface collapses into a pocket, indicating the opening of the PG.

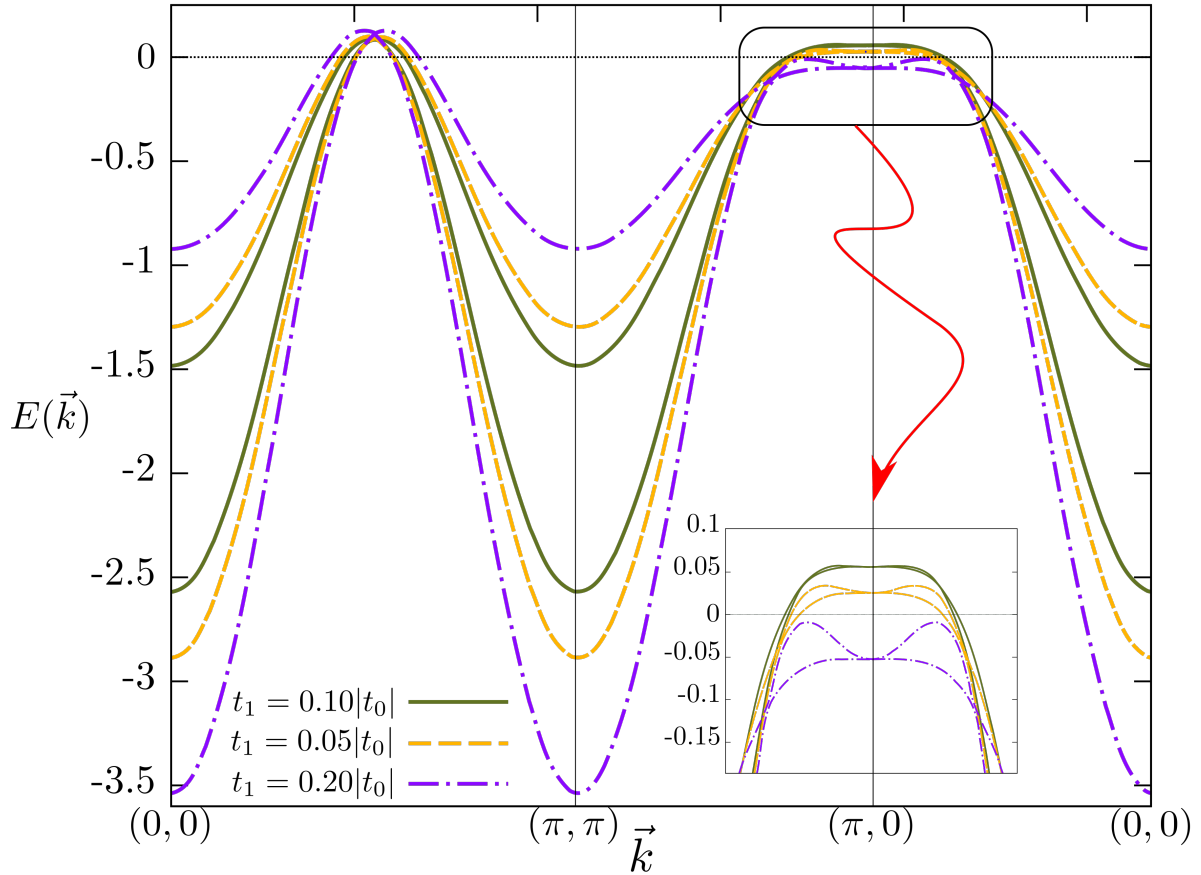


**Figure 2.** Energy bands for the normal state with  $U = 9.0|t_0|$ ,  $n_T = 0.90$ ,  $k_B T = 0.05|t_0|$  for  $t_1 = 0.05|t_0|$ ,  $t_1 = 0.10|t_0|$  and  $t_1 = 0.20|t_0|$ . The dotted black line indicates the position of the chemical potential.

Figure 1 shows the FS for different values of  $t_1$  in the normal state. Panels (a) and (b) show two competing topologies for the FS, originating from the superposition of two bands with  $\mu$ . Panel (c) illustrates the FS collapsed into a pocket, indicating

that the PG is open. The band shift  $Y_{\vec{k},\sigma}$  is affected in a more significant manner by  $t_1$ , enhancing the short-range antiferromagnetic correlations on the nodal point  $(\pi, \pi)$  and on the anti-nodal point  $(\pi, 0)$ . This is evident in figure 2, as a band displacement to lower energy levels characterizes the distortion. The collapse into a pocket indicates that an increase in the short-range antiferromagnetic correlations caused by  $t_1$  is responsible for the opening of the PG. The mechanism is characterized by a distortion of the bands on the anti-nodal point  $(\pi, 0)$ , which gets further displaced to lower energies, until both bands are below  $\mu$ , thus, opening the PG, this is evident in the insert, which is a close-up view of the bands close to  $\mu$  on the  $(\pi, 0)$  point. Furthermore,  $t_1$  also distorts the bands on the nodal point  $(\pi, \pi)$  in a similar manner, in this case, one of the bands gets displaced to further lower energies, while the other approaches  $\mu$ .

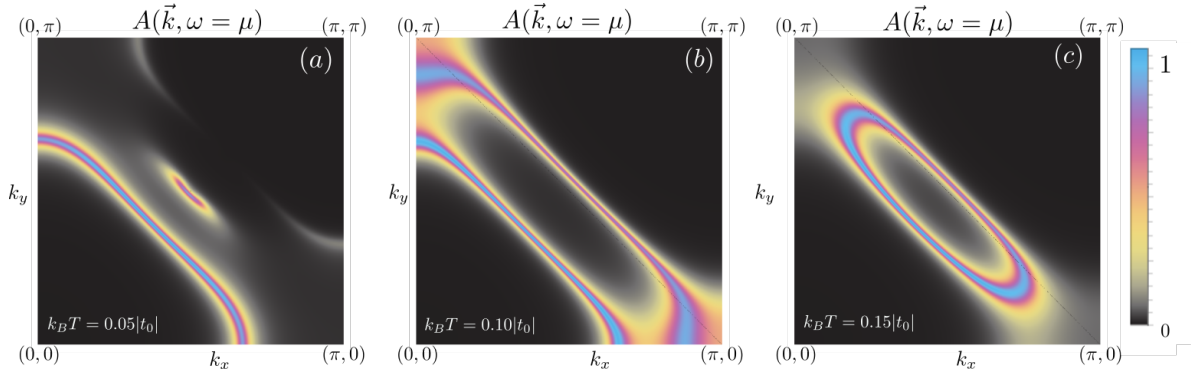


**Figure 3.** (a) Reconstructed Fermi surface in the CDW phase due to antiferromagnetic correlations for  $k_B T = 0.05|t_0|$ . Normal state Fermi surfaces, (b) for  $k_B T = 0.10$  and (c)  $k_B T = 0.15$ , with  $U = 16|t_0|$ ,  $n_T = 0.90$ ,  $t_1 = 0.12|t_0|$ . In panel (c), the FS collapses into a pocket, indicating the opening of the PG. The dotted black line indicates the position of the chemical potential.

Figure 3 shows the FS evolution with  $k_B T$ . We have a fully-fledged reconstructed electron-like surface in the CDW phase on panel (a). On panel (b), the thickness of the lines in the boundary regions of the Brillouin zone predicts a change in the Fermi surface topology, in this case, the collapse into a pocket. Indeed, this is observed in panel (c), where an increase in  $k_B T$  leads to the opening of the PG, characterized by the collapse of the FS into a pocket. The electron-like topology presented here comes from the strong antiferromagnetic correlations, differing from the expected behavior of a total surface collapse. This reconstruction suggests that even within the CDW phase, the correlations play a relevant role.

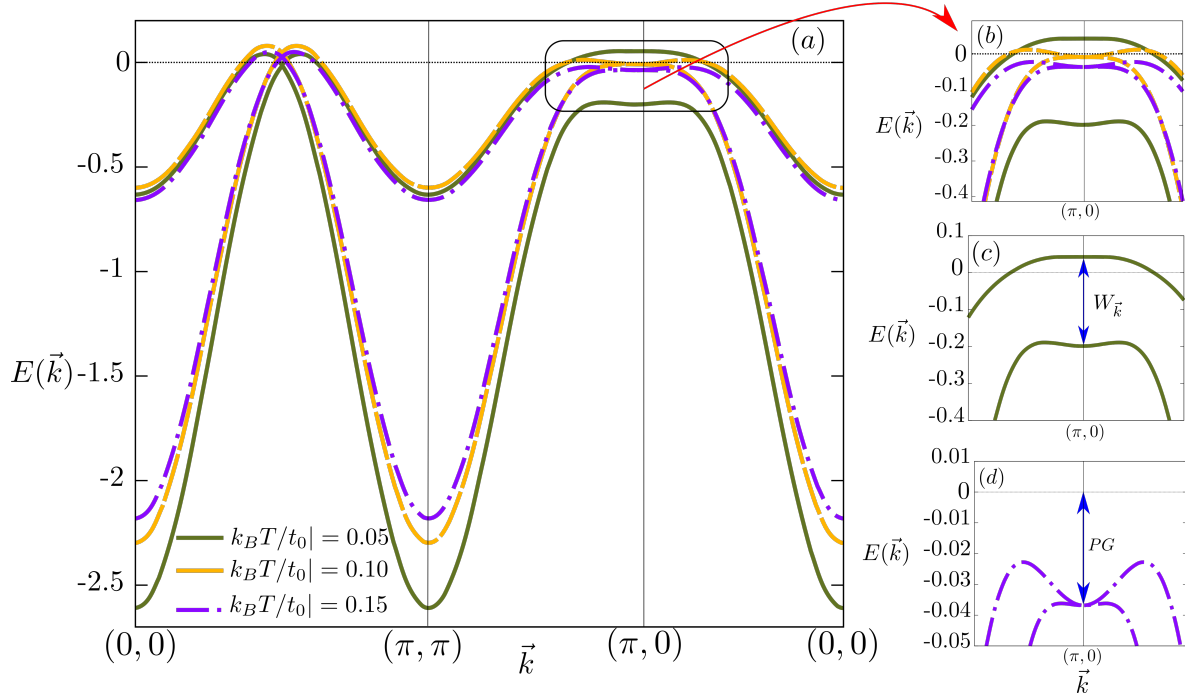


**Figure 4.** (a) Energy bands for  $k_B T = 0.05|t_0|$ ,  $k_B T = 0.10|t_0|$  and  $k_B T = 0.15|t_0|$ , with  $U = 16.0|t_0|$ ,  $n_T = 0.90$ ,  $t_1 = 0.12|t_0|$ . (b) Close-up view of the bands close to the chemical potential level on the anti-nodal point  $(\pi, 0)$ , (c) Close-up view of the CDW gap opening on the  $(\pi, 0)$  point, for  $k_B T = 0.05|t_0|$ . (d) Close-up view of the pseudogap, on the  $(\pi, 0)$  point, for  $k_B T = 0.15|t_0|$ . The dotted black line indicates the position of the chemical potential.

Figure 4 displays the energy bands corresponding to the FS in figure 3. The opening of the CDW gap happens on the anti-nodal point  $(\pi, 0)$ , for  $k_B T = 0.05|t_0|$ . There is a degeneracy lifting, that splits the bands on this point, opening the gap.  $Y_{\vec{k}, \sigma}$  heavily distorted the bands in the nodal points, displacing those to regions below  $\mu$ . The band region around the nodal point  $(\pi, 0)$  is distorted in the same way as in the nodal point  $(\pi, \pi)$ , this was caused by the effects of  $Y_{\vec{k}, \sigma}$ . The PG is observed when  $k_B T = 0.15|t_0|$ , as the bands do not cross  $\mu$  in  $(\pi, 0)$ . However, intersections still occur at  $(\pi/2, \pi/2)$ , meaning the gap is partial. In figure 4 panel (c),  $k_B T = 0.05|t_0|$ . The CDW gap opening happens in the same region as the PG. The shift of the upper band to an energy region above  $\mu$  breaks the degeneracy introduced by the periodicity of the lattice. The occurrence of both effects in the same point of the first Brillouin zone complicates the separate analysis, as within the ordered phase, the effects of the PG are no longer as clear. Figure 4 panel (d) represents the case when  $k_B T = 0.15|t_0|$ . The difficulty in analyzing the relation between CDW and the PG lies in the superposition of their effects on the electronic structure of the system. The PG and the CDW gap open on the anti-nodal point  $(\pi, 0)$ . Therefore, any indicative information about the PG is lost with the gap opening. However, the band shift causes the two lower bands to be completely localized below  $\mu$  at the point  $(\pi, 0)$ . Thus, the gap opening causes a degeneracy breaking at this point, separating the bands and giving rise to the CDW. The gap is the distance

between the two band values at this  $\vec{k}$  point. Nevertheless, the flatness of this region is kept after the splitting. This suggests that there are still localized electronic states, reminiscent of the normal state. We can see that this degeneracy breaking leads to an intersection between  $\mu$  and the upper band, reconstructing the FS.

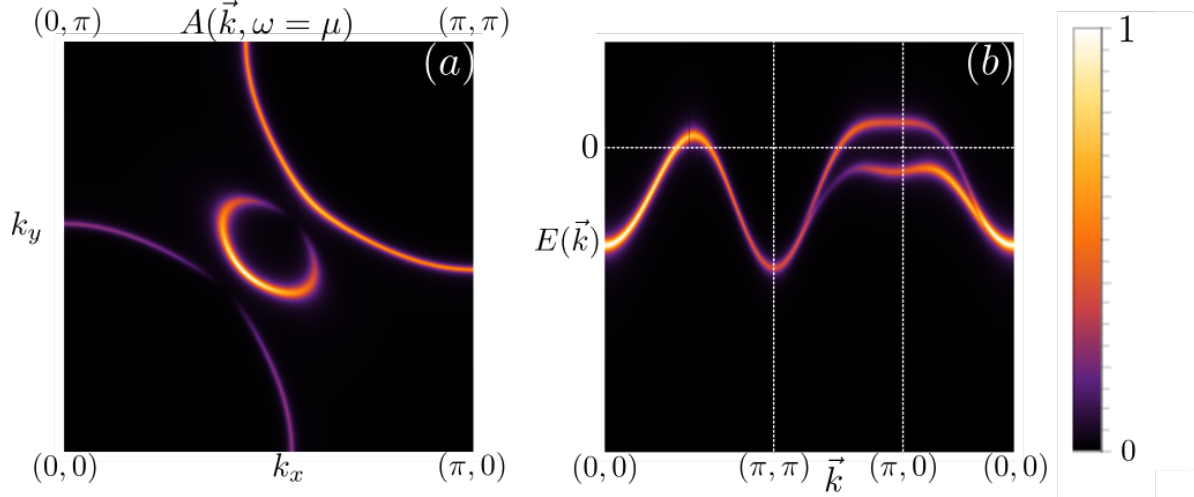


**Figure 5.** (a) Fermi surface reconstructed by antiferromagnetic correlations in the CDW phase. (b) Energy bands near the chemical potential level are calculated using the spectral function along the high-symmetry path of the reduced first Brillouin zone, with  $U = 16.0|t_0|$ ,  $n_T = 0.85$  and  $t_1 = 0.1|t_0|$ . The dotted white line indicates the position of the chemical potential.

In Figure 5 panel (a), there is a shadow band effect happening, characterized by a much smaller intensity FS, originating from the proximity of the antiferromagnetic state [67]. In panel (b), a luminosity maximum is observed in the regions around the  $(0,0)$  point, and around the CDW gap region, near the  $(\pi,0)$  region. This indicates the effects of the short-range antiferromagnetic correlations within the CDW phase, suggesting a connection between the PG phenomenon and CDW. Similar behavior is illustrated in figure 6, but the system is now in a regime of stronger correlations, as  $n_T = 0.90$ . However, the luminosity distribution in the bands follows the same pattern as in the case of  $n_T = 0.85$ . The reconstructed FS undergoes a LT, indicating that the antiferromagnetic correlations are intense enough to cause it within the CDW phase.

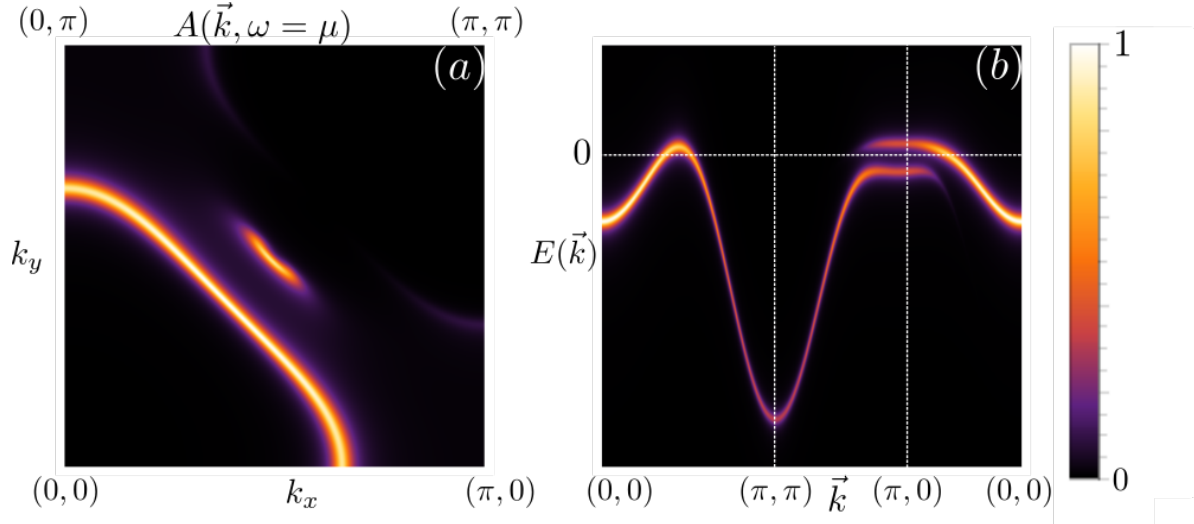


**Figure 6.** (a) Fermi surface reconstructed by antiferromagnetic correlations in the CDW phase. (b) Energy bands near the chemical potential level are calculated using the spectral function along the high-symmetry path of the reduced first Brillouin zone, with  $U = 16.0|t_0|$ ,  $n_T = 0.90$  and  $t_1 = 0.1|t_0|$ . The dotted white line indicates the position of the chemical potential.

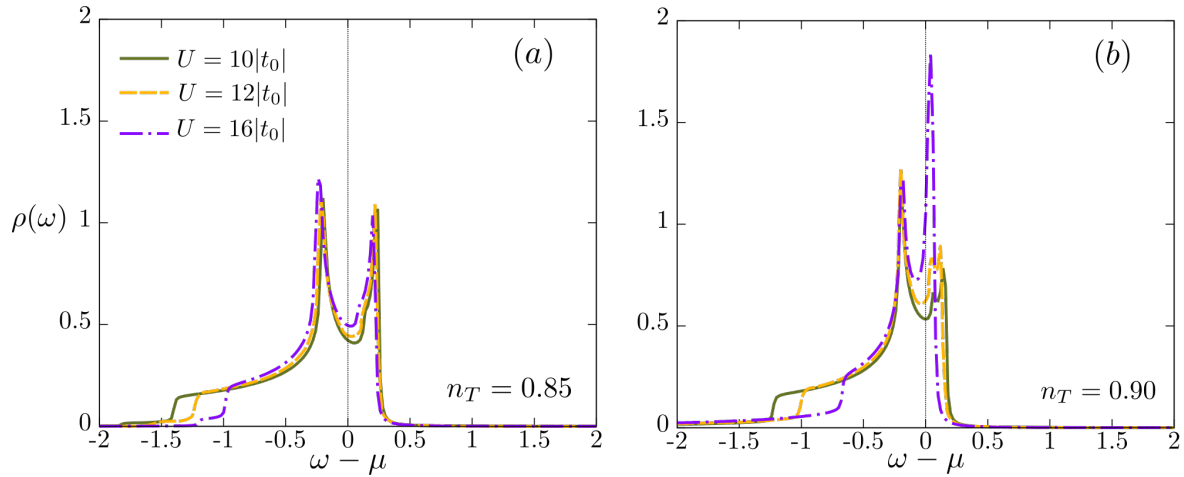


**Figure 7.** The density of states in the CDW phase for  $U = 10|t_0|$ ,  $U = 12|t_0|$  and  $U = 16|t_0|$ , shown under (a)  $n_T = 0.85$  and (b)  $n_T = 0.90$ , at  $k_B T = 0.05|t_0|$  and  $t_1 = 0.1|t_0|$ . The dotted black line indicates the position of the chemical potential.

To investigate the consequences of this LT, the DOS for  $n_T = 0.85$  and  $n_T = 0.90$  is analyzed in Figure 7. A VHS, shifted from  $\mu$ , is illustrated. In other words, there is a reduction in accessible states for the stability of the CDW phase, as the peak of the VHS does not align with  $\mu$ . In Figure 4, the PG and the CDW gap occur in the same first Brillouin zone region, indicating an intertwining between the phenomena, caused by a regime of strong correlations, since  $U = 16.0|t_0|$  corresponds to twice the system's bandwidth. Indeed, the effects of  $k_B T$  are pivotal in our theory. For

$k_B T^* \geq k_B T > k_B T_C$ , the DOS assumes a one-peak structure, which can get displaced by  $t_1$ . For  $k_B T < k_B T_C$  there is a rise of a second, smaller VHS-like peak, separated by a partial gap in the DOS. This indicates the opening of the CDW, as there is a gap between both peaks. The effects of the short-range antiferromagnetic correlations cause a piling of states on  $\mu$ , further emphasizing a connection with the PG, as the expected behavior would be a total gap.

The order parameter  $W_{\vec{k}}$  is calculated as a function of  $n_T$  for different values of  $U$ , see figure 8 panel (a). An initial favoring is followed by suppression in the order parameter amplitude, caused by increasing  $n_T$ . This implies an optimal correlation regime for  $0.75 \gtrsim n_T \gtrsim 0.85$ , where the antiferromagnetic correlations favor CDW stability. For the specific case with  $U = 16.0|t_0|$ , the LT precedes the onset of the CDW collapse. In this result,  $k_B T$  was kept fixed; however, at higher  $k_B T$ , the PG opens. Thus, assuming the change in the density of states structure, the suppression of  $W_{\vec{k}}$ , and the change in the FS topology, it is inferred that at low  $k_B T$  and strong antiferromagnetic correlations, there is an intertwining between CDW and the PG.

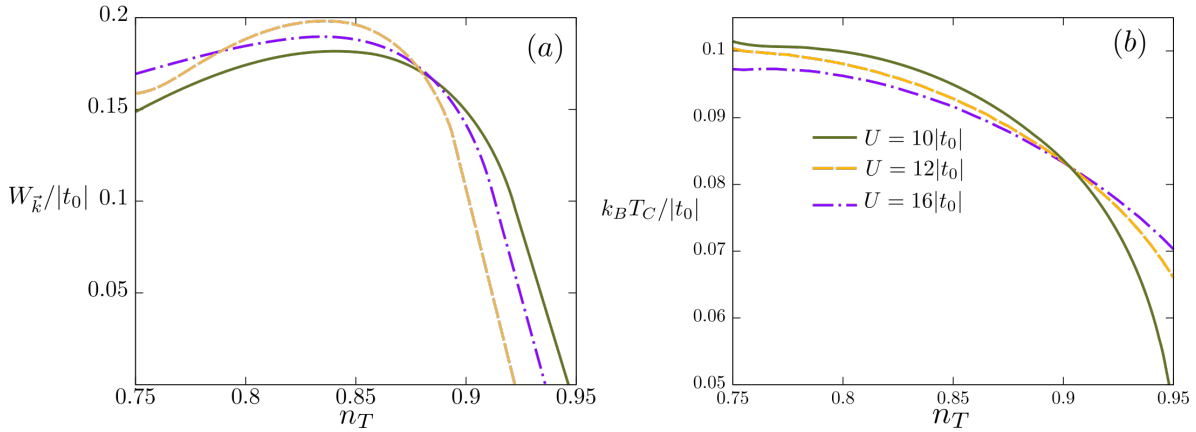


**Figure 8.** (a) CDW order parameter and (b) critical temperature as a function of  $n_T$  for  $U = 10|t_0|$ ,  $U = 12|t_0|$  and  $U = 16|t_0|$ , with  $t_1 = 0.1|t_0|$  and  $k_B T = 0.05|t_0|$ .

To further investigate the CDW regime,  $k_B T_C$  as a function of  $n_T$  is analyzed for various values of  $U$  in Figure 8, panel (b). The increase in  $n_T$  causes a suppression in  $k_B T_C$ , particularly pronounced for more intense correlation regimes. Notably, for  $U = 16.0|t_0|$ , the decay of  $k_B T_C$  is more pronounced, emphasizing the connection between CDW and the PG. Supporting the previously mentioned optimal correlations regime, the behavior of  $k_B T_C$  reflects what was stated in panel (a). This optimal regime happens in the  $0.75 \gtrsim n_T \gtrsim 0.85$  interval, before the LT, at  $n_T = 0.90$ . The collapse of the CDW occurring in the vicinity of the LT, supports the intertwining of the PG and the CDW, as it was previously stated that the onset of the PG is related to the LT.

As seen earlier,  $t_1$  can also lead to the opening of the PG. To analyze its effect, the order parameter is calculated as a function of  $t_1$  for different  $n_T$ , as shown in Figure 9 panel (a). For  $n_T = 0.80$  and  $n_T = 0.85$ , there is a steady increase in the order parameter, emphasizing the existence of two regimes, mediated by the intensity of the

short-range antiferromagnetic correlations. This is associated with the displacement of states to regions near  $\mu$ , which cease to contribute to the CDW phase. For  $n_T = 0.90$ , the CDW suppressive effects of increasing  $t_1$  are more relevant, indicating that the number of accessible states near  $\mu$  has decreased, as  $t_1$  distorts not only the bands but also the position of the VHS peak. This is reinforced by the difference in the gap amplitude by the decay for  $t_1/|t_0| \gtrsim 0.07$ , indicating the possible opening of the PG for slightly more intense correlations or  $k_B T$ . Finally,  $k_B T_C$  as a function of  $t_1/|t_0|$  is analyzed in Figure 9 panel (b). For higher values of  $t_1$ , there is an inversion in the amplitude of  $T_C$ , reinforcing the existence of an optimal correlation regime. For  $U = 16.0|t_0|$ , suppressive effects occur for smaller values of  $t_1$  in a more pronounced behavior. The PG and CDW are connected through antiferromagnetic correlations. These initially favor the ordered phase, but when sufficiently intense, tend to suppress the CDW and change the topology of the FS, which after the LT, collapses into a pocket, showing that the PG is open.

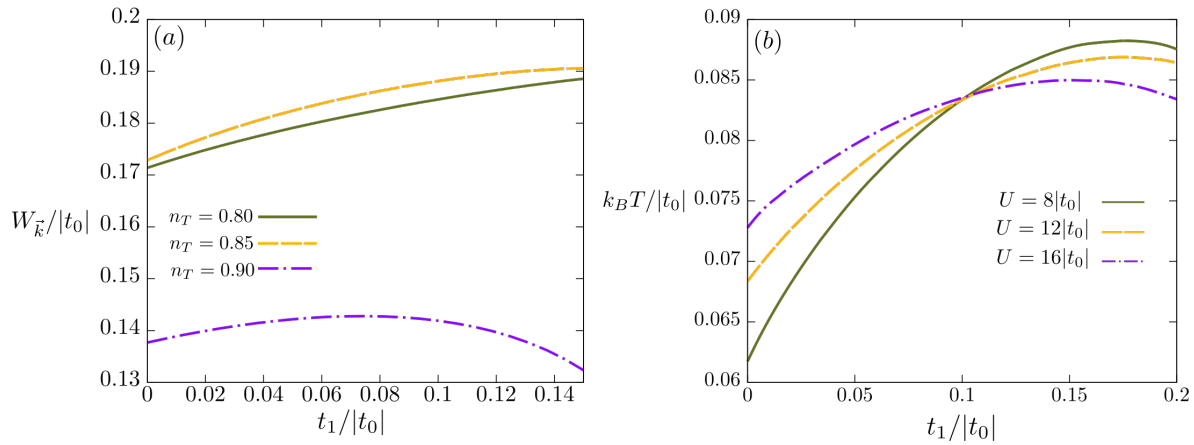


**Figure 9.** (a) CDW order parameter with  $k_B T = 0.05|t_0|$  and  $U = 12|t_0|$ , for  $n_T = 0.80$ ,  $n_T = 0.85$  and  $n_T = 0.90$ . (b) CDW critical temperature at  $n_T = 0.90$ , as a function of  $t_1$  for  $U = 10|t_0|$ ,  $U = 12|t_0|$  and  $U = 16|t_0|$ .

## 4. Conclusions

We employed a BCS-like mean field approximation, within the Green's function equation of motion formalism to describe the CDW instability. We replaced the normal state uncorrelated Green's functions with a correlated one, obtained through the n-pole approximation applied to the single-band Hubbard model. This has been done considering next-nearest neighbors  $t_1$ , that along  $n_T$  and  $U$ , act on the spin-spin correlation  $\langle \vec{S}_i \cdot \vec{S}_j \rangle$ , strongly affecting the band shift  $Y_{\vec{k},\sigma}$ . We emphasize that  $Y_{\vec{k},\sigma}$  acquires a structure in the reciprocal space that enhances such correlations. Remarkably, the effect becomes relevant at anti-nodal point  $(\pi, 0)$  as discussed below. It is important to mention that generally, the correlation functions in the band shift do not have an explicit dependence on the reciprocal space [41, 44]. This dependence displaces the bands in the nodal point  $(\pi, \pi)$  and the anti-nodal point  $(\pi, 0)$  to lower energy regions.

For  $t_1$  sufficiently large, the entire region around  $(\pi, 0)$  is distorted, which is responsible for the opening of the PG.

The VHS peak can be displaced by  $n_T$  and  $t_1$ , which triggers a LT, favoring the onset of the PG since the DOS presents a change in shape. This deformation reorganizes states, resulting in their suppression in the region around  $\mu$  and accumulation near the VHS peak. In other words, both the LT and the PG can be induced by short-range antiferromagnetic correlations [68, 69]. When  $k_B T$  is lowered, the DOS assumes a two-peak structure. The superposition of the main VHS peak with  $\mu$ , creates an abundance of accessible states, further stabilizing the CDW as given by the order parameter behavior. Nevertheless, the FS is reconstructed due to the opening of the CDW gap, which deforms the bands, allowing the intersection of  $\mu$  with the upper band at this anti-nodal point. Ultimately, this deformation comes from the dependence on  $\vec{k}$  of the band shift which enhances short-range antiferromagnetic correlations at  $(\pi, 0)$ . For  $k_B T \gg k_B T_C$ , within a specific range of  $n_T$  and  $U$ , the displacement of the VHS peak along the energy axis caused by  $Y_{\vec{k},\sigma}$  can be either beneficial or harmful to the electron-hole pair formation. The states displaced away from  $\mu$  stop contributing to pair formation. We highlight the presence of a LT within the ordered phase, triggered by an increase in  $n_T$ , further emphasizing the importance of this analysis, since the VHS peak position was displaced to higher energies.

In conclusion, we have proposed a theory, where the short-range antiferromagnetic correlations constitute its cornerstone, to describe the connection between CDW and the PG. We explored the connections between the PG and the FS reconstruction within the CDW phase through the band distortions caused by such correlations. The VHS originated from the flat region on the anti-nodal point  $(\pi, 0)$  exerts a fundamental role, by triggering a LT, but also being able to suppress and benefit the ordered phase. The role of the VHS is a direct consequence of the short-range antiferromagnetic correlations [70, 71]. We mention results from cuprates where a LT precedes the onset of the PG [72, 73, 74] and the FS reconstruction coexisting with Fermi arcs [75, 76]. In the latter case, we have a fully formed Fermi surface, which coexists with an unstable Fermi arc spread on the anti-nodal line.

## References

- [1] Chen S D, Hashimoto M, He Y, Song D, He J F, Li Y F, Ishida S, Eisaki H, Zaanen J, Devereaux T P, Lee D H, Lu D H and Shen Z X 2022 *Nature* **601**(7894) 562–567 ISSN 14764687
- [2] Bejas M, Buzon G, Greco A and Foussats A 2011 *Phys. Rev. B* **83**(1) 014514 URL <https://link.aps.org/doi/10.1103/PhysRevB.83.014514>
- [3] Bonetti P M, Mitscherling J, Vilaridi D and Metzner W 2020 *Physical Review B* **101**(16) ISSN 24699969
- [4] Chan M K, Harrison N, McDonald R D, Ramshaw B J, Modic K A, Barišc N and Greven M 2016 *Nature Communications* **7** ISSN 20411723
- [5] Doiron-Leyraud N, Badoux S, Cotret S R D, Lepault S, Leboeuf D, Laliberté F, Hassinger E, Ramshaw B J, Bonn D A, Hardy W N, Liang R, Park J H, Vignolles D, Vignolle B, Taillefer L and Proust C 2015 *Nature Communications* **6** ISSN 20411723

- [6] Eberlein A, Metzner W, Sachdev S and Yamase H 2016 *Physical Review Letters* **117**(18) ISSN 10797114
- [7] Fang Y, Grissonnanche G, Legros A, Verret S, Laliberté F, Collignon C, Ataei A, Dion M, Zhou J, Graf D, Lawler M J, Goddard P A, Taillefer L and Ramshaw B J 2022 *Nature Physics* **18**(5) 558–564 ISSN 17452481
- [8] Ivantsov I, Ferraz A and Kochetov E 2018 *Physical Review B* **98**(21) ISSN 24699969
- [9] Keimer B, Kivelson S A, Norman M R, Uchida S and Zaanen J 2015 *Nature* **518**(7538) 179–186 ISSN 14764687
- [10] Li L J, O’Farrell E C, Loh K P, Eda G, Özyilmaz B and Neto A H C 2016 *Nature* **529**(7585) 185–189 ISSN 14764687
- [11] Bovet M, Popović D, Clerc F, Koitzsch C, Probst U, Bucher E, Berger H, Naumović D and Aebi P 2004 *Physical Review B - Condensed Matter and Materials Physics* **69**(12) ISSN 1550235X
- [12] Singh B, Hsu C H, Tsai W F, Pereira V M and Lin H 2017 *Physical Review B* **95**(24) ISSN 24699969
- [13] Chen C, Singh B, Lin H and Pereira V M 2018 *Physical Review Letters* **121**(22) ISSN 10797114
- [14] Hu Q, Liu J Y, Shi Q, Zhang F J, Zhong Y, Lei L and Ang R 2021 *EPL* **135**(5) ISSN 12864854
- [15] Levy-Bertrand F, Michon B, Marcus J, Marcenat C, Kačmarčík J, Klein T and Cercellier H 2016 *Physica C: Superconductivity and its Applications* **523** 19–22 ISSN 09214534
- [16] Lian C S, Si C and Duan W 2018 *Nano Letters* **18**(5) 2924–2929 ISSN 15306992
- [17] Zhang M, Zhang Y, Guo H and Yang F 2021 *Chinese Physics B* **30**(10) ISSN 20583834
- [18] Zhang J, Phelan D, Botana A S, Chen Y S, Zheng H, Krogstad M, Wang S G, Qiu Y, Rodriguez-Rivera J A, Osborn R, Rosenkranz S, Norman M R and Mitchell J F 2020 *Nature Communications* **11**(1) ISSN 20411723
- [19] Li Y, Balédent V, Barišić N, Cho Y, Fauqué B, Sidis Y, Yu G, Zhao X, Bourges P and Greven M 2008 *Nature* **455**(7211) 372–375 ISSN 14764687
- [20] Fauqué B, Sidis Y, Hinkov V, Pailhès S, Lin C T, Chaud X and Bourges P 2006 *Physical Review Letters* **96**(19) ISSN 00319007
- [21] Krien F, Worm P, Chalupa-Gantner P, Toschi A and Held K 2022 *Communications Physics* **5** 336
- [22] Singh D K, Kadge S, Bang Y and Majumdar P 2022 *Physical Review B* **105**(5) ISSN 24699969  
aqui tem o valor esperado para a utilização de  $V$ , e  $U$
- [23] Bounoua D, Sidis Y, Loew T, Bourdarot F, Boehm M, Steffens P, Mangin-Thro L, Balédent V and Bourges P 2022 *Communications Physics* **5** 268
- [24] Anderson P W, Lee P, Randeria M, Rice T, Trivedi N and Zhang F 2004 *Journal of Physics: Condensed Matter* **16** R755
- [25] Punk M, Allais A and Sachdev S 2015 *Proceedings of the National Academy of Sciences* **112** 9552–9557
- [26] Sakai S, Civelli M and Imada M 2016 *Physical review letters* **116** 057003
- [27] Lee P A, Nagaosa N and Wen X G 2006 *Reviews of modern physics* **78** 17
- [28] Yang K Y, Rice T and Zhang F C 2006 *Physical Review B* **73** 174501
- [29] Doiron-Leyraud N, Cyr-Choinière O, Badoux S, Ataei A, Collignon C, Gourgout A, Dufour-Beauséjour S, Tafti F F, Laliberté F, Boulanger M E, Matusiak M, Graf D, Kim M, Zhou J S, Momono N, Kurosawa T, Takagi H and Taillefer L 2017 *Nature Communications* **8**(1) ISSN 20411723
- [30] Xiao B, He Y Y, Georges A and Zhang S 2023 *Physical Review X* **13**(1) ISSN 21603308
- [31] Rosen J A, Comin R, Levy G, Fournier D, Zhu Z H, Ludbrook B, Veenstra C N, Nicolaou A, Wong D, Dosanjh P, Yoshida Y, Eisaki H, Blake G R, White F, Palstra T T, Sutarto R, He F, Pereira A F, Lu Y, Keimer B, Sawatzky G, Petaccia L and Damascelli A 2013 *Nature Communications* **4** ISSN 20411723
- [32] Sachdev S and Placa R L 2013 *Physical Review Letters* **111**(2) ISSN 00319007
- [33] Leboeuf D, Doiron-Leyraud N, Vignolle B, Sutherland M, Ramshaw B J, Levallois J, Daou R, Laliberté F, Cyr-Choinière O, Chang J, Jo Y J, Balicas L, Liang R, Bonn D A, Hardy W N,

- Proust C and Taillefer L 2011 *Physical Review B - Condensed Matter and Materials Physics* **83**(5) ISSN 10980121
- [34] Norman M R, Lin J and Millis A J 2010 *Physical Review B - Condensed Matter and Materials Physics* **81**(18) ISSN 10980121
- [35] Miao H, Fabbri G, Koch R J, Mazzone D G, Nelson C S, Acevedo-Esteves R, Gu G D, Li Y, Yilmaz T, Kaznatcheev K, Vescovo E, Oda M, Kurosawa T, Momono N, Assefa T, Robinson I K, Bozin E S, Tranquada J M, Johnson P D and Dean M P 2021 *npj Quantum Materials* **6**(1) ISSN 23974648
- [36] Tabis W, Li Y, Tacon M L, Braicovich L, Kreyssig A, Minola M, Dellea G, Weschke E, Veit M, Ramazanoglu M *et al.* 2014 *Nature communications* **5** 5875
- [37] Regmi S, Bin Elius I, Sakhya A P, Jeff D, Sprague M, Mondal M I, Jarrett D, Valadez N, Agosto A, Romanova T *et al.* 2023 *Scientific Reports* **13** 18618
- [38] Kawasaki S, Li Z, Kitahashi M, Lin C T, Kuhns P L, Reyes A P and Zheng G Q 2017 *Nature Communications* **8**(1) ISSN 20411723
- [39] Klett M, Hansmann P and Schäfer T 2022 *Frontiers in Physics* **10** ISSN 2296424X
- [40] Zhang K W, Yang C L, Lei B, Lu P, Li X B, Jia Z Y, Song Y H, Sun J, Chen X, Li J X and Li S C 2018 *Science Bulletin* **63**(7) 426–432 ISSN 20959281
- [41] Roth L M 1969 *Physical Review* **184** 451
- [42] Calegari E and Rodríguez-Núñez J 2016 *Physics Letters A* **380** 495–501 ISSN 0375-9601 URL <http://www.sciencedirect.com/science/article/pii/S0375960115009512>
- [43] Hubbard J 1963 *Proc. Roy. Soc. A* **276** 238–257
- [44] Beenen J and Edwards D 1995 *Physical Review B* **52** 13636
- [45] Calegari E, Magalhaes S and Gomes A 2005 *The European Physical Journal B-Condensed Matter and Complex Systems* **45** 485–496
- [46] Calegari E and Magalhaes S 2011 *International Journal of Modern Physics B* **25** 41–53
- [47] Shneyder E I, Zotova M V, Nikolaev S V and Ovchinnikov S G 2021 *Phys. Rev. B* **104**(15) 155153 URL <https://link.aps.org/doi/10.1103/PhysRevB.104.155153>
- [48] Grandadam M, Chakraborty D, Montiel X and Pépin C 2020 *Phys. Rev. B* **102**(12) 121104 URL <https://link.aps.org/doi/10.1103/PhysRevB.102.121104>
- [49] Markiewicz R S, Sahrakorpi S, Lindroos M, Lin H and Bansil A 2005 *Physical Review B - Condensed Matter and Materials Physics* **72**(5) ISSN 10980121
- [50] Scheurer M S, Chatterjee S, Wu W, Ferrero M, Georges A and Sachdev S 2018 *Proceedings of the National Academy of Sciences of the United States of America* **115**(16) E3665–E3672 ISSN 10916490
- [51] Zhang L, Zhong Y and Luo H G 2020 *Chinese Physics B* **29**(7) ISSN 20583834
- [52] Gao J, Park J W, Kim K, Song S K, Park H R, Lee J, Park J, Chen F, Luo X, Sun Y *et al.* 2020 *Nano Letters* **20** 6299–6305
- [53] Tu W L and Lee T K 2019 *Scientific Reports* **9**(1) ISSN 20452322
- [54] Atkinson W A, Ufkens S and Kampf A P 2018 *Physical Review B* **97**(12) ISSN 24699969
- [55] Davis J C and Lee D H 2013 *Proceedings of the National Academy of Sciences of the United States of America* **110**(44) 17623–17630 ISSN 00278424
- [56] McMahon C, Achkar A J, Da E H, Neto S, Djianto I, Menard J, He F, Sutarto R, Comin R, Liang R, Bonn D A, Hardy W N, Damascelli A and Hawthorn D G 2020 Orbital symmetries of charge density wave order in  $\text{YBa}_2\text{Cu}_3\text{O}_{6+x}$  URL <https://www.science.org>
- [57] Fujita K, Hamidian M H, Edkins S D, Kim C K, Kohsaka Y, Azuma M, Takano M, Takagi H, Eisaki H, Uchida S *et al.* 2014 *Proceedings of the National Academy of Sciences* **111** E3026–E3032
- [58] Blackburn E, Chang J, Hücker M, Holmes A, Christensen N B, Liang R, Bonn D, Hardy W, Rütt U, Gutowski O *et al.* 2013 *Physical review letters* **110** 137004
- [59] Guster B, Canadell E, Pruneda M and Ordejón P First principles analysis of the cdw instability of single-layer  $1t\text{-TiSe}_2$  and its evolution with charge carrier density
- [60] Chen P, Chan Y H, Fang X Y, Zhang Y, Chou M Y, Mo S K, Hussain Z, Fedorov A V and Chiang

- T C 2015 *Nature Communications* **6** ISSN 20411723
- [61] Burian M, Porer M, Mardegan J R, Esposito V, Parchenko S, Burganov B, Gurung N, Ramakrishnan M, Scagnoli V, Ueda H, Francoual S, Fabrizio F, Tanaka Y, Togashi T, Kubota Y, Yabashi M, Rossnagel K, Johnson S L and Staub U 2021 *Physical Review Research* **3**(1) ISSN 26431564
- [62] Miao H, Ishikawa D, Heid R, Le Tacon M, Fabbris G, Meyers D, Gu G D, Baron A Q R and Dean M P M 2018 *Phys. Rev. X* **8**(1) 011008 URL <https://link.aps.org/doi/10.1103/PhysRevX.8.011008>
- [63] Heumen E V, Muhlethaler E, Kuzmenko A B, Eisaki H, Meevasana W, Greven M and Marel D V D 2009 *Physical Review B - Condensed Matter and Materials Physics* **79**(18) ISSN 10980121
- [64] Balseiro C A and Falicov L M 1979 *Phys. Rev. B* **20**(11) 4457–4464 URL <https://link.aps.org/doi/10.1103/PhysRevB.20.4457>
- [65] Zubarev D N 1960 *Soviet Physics Uspekhi* **3** 320
- [66] Avella A and Mancini F 2007 *Physical Review B* **75** 134518
- [67] Vilk Y 1997 *Physical Review B* **55** 3870
- [68] Bragança H, Sakai S, Aguiar M C O and Civelli M 2018 *Physical review letters* **120**(6) 67002
- [69] Wu W, Scheurer M S, Chatterjee S, Sachdev S, Georges A and Ferrero M 2018 *Physical Review X* **8**(2) ISSN 21603308
- [70] Paul I and Civelli M 2023 *Physical Review B* **107**(20) ISSN 24699969
- [71] Bonetti P M and Metzner W 2022 *Physical Review B* **106**(20) ISSN 24699969
- [72] Benhabib S, Sacuto A, Civelli M, Paul I, Cazayous M, Gallais Y, Méasson M A, Zhong R D, Schneeloch J, Gu G D, Colson D and Forget A 2015 *Physical Review Letters* **114**(14) ISSN 10797114
- [73] Ino A, Kim C, Nakamura M, Yoshida T, Mizokawa T, Fujimori A, Shen Z X, Kakeshita T, Eisaki H and Uchida S 2002 *Physical Review B* **65** 094504
- [74] Piriou A, Jenkins N, Berthod C, Maggio-Aprile I and Fischer Ø 2011 *Nature communications* **2** 221
- [75] Meng J, Liu G, Zhang W, Zhao L, Liu H, Jia X, Mu D, Liu S, Dong X, Zhang J, Lu W, Wang G, Zhou Y, Zhu Y, Wang X, Xu Z, Chen C and Zhou X J 2009 *Nature* **462**(7271) 335–338 ISSN 00280836
- [76] Tam C C, Zhu M, Ayres J, Kummer K, Yakhov-Harris F, Cooper J R, Carrington A and Hayden S M 2022 *Nature Communications* **13**(1) ISSN 20411723